DOI 10.1007/s10527-016-9603-5
Biomedical Engineering, Vol. 50, No. 2, July, 2016, pp. 128-133. Translated from Meditsinskaya Tekhnika, Vol. 50, No. 2, Mar.-Apr., 2016, pp. 40-44.
Original article submitted January 28, 2016.

Designing a Mechanotherapy Device for Rehabilitation of Lower Extremities of Humans

S. M. Jatsun[1], A. S. Jatsun[2], and A. N. Rukavitsyn[2]*

An approach to designing a mechanotherapeutic device for rehabilitation of lower extremities in humans using numerical simulation of dynamic processes taking place in the device is described. The device is based on a multilink biomechatronic device with linear actuators.

Introduction

Paralysis of extremities (especially lower) in humans is not a static condition, but a dynamic process with two phases of the death of nerve cells in the patient – necrosis and apoptosis.

The ability to restore motor function in patients with paralysis of the lower or upper limbs was identified quite recently. Thus, it was found that the human spinal cord contains neurons capable of producing stepping patterns that control leg motions. This network of neurons can be activated using electrical stimulation of the spinal cord [1, 2]. It is known that mechanical stimulation of support zones of the feet in the mode of natural locomotion controls the ratio of activity of postural and phase muscles of motor movement [3]. Laboratory studies have shown that periodic stimulation of afferent neurons of the lower extremities leads to start of a stepping generator and ensures the safety of motor neurons below the level of injury [4].

Hence, it is well established that locomotor trainings can be used in the rehabilitation of patients with damage of the musculoskeletal system. Forced limb movements are implemented using a new generation of biotraining equipment with active actuators, necessary sensing, and with means for stimulation of the patient using advanced software. Such biomechatronic sports and medical training machines are already produced abroad. In Russia, despite the high demand for these devices, there have been only a few attempts to develop such machines [5, 6].

Materials and Methods

Numerical simulation and analysis of the behavior of a developed biomechatronic rehabilitation system for patient verticalization when moving from "sitting" to "standing" are needed to determine parameters of controlled motion of the four-link mechanism with active hip, knee, and ankle joints. In this case, the main task of the study was to determine the range of motion done by the links that were performing angular movements along predetermined trajectories.

The simulation was performed in two stages: the first stage defined dynamic parameters of motion of the links and characteristics of actuators of the joints in the "rising" mode. In the second stage, the resulting model was complemented by real geometry of the actuators and connecting elements of the construction [7, 8]. For mathematical modeling of the biomechatronic device, the latter was assumed a mechanical multilink system consisting of four solid links connected by rotary joints (Fig. 1a).

For the numerical description of the motion of the system of bodies in the verticalization mode, the system was presented in the form of a kinematic chain consisting of links 1-4. This makes the following assumptions: (i) all

[1] Kursk State University, Kursk, Russia.
[2] Southwestern State University, Kursk, Russia; E-mail: alruk75@mail.ru
* To whom correspondence should be addressed.

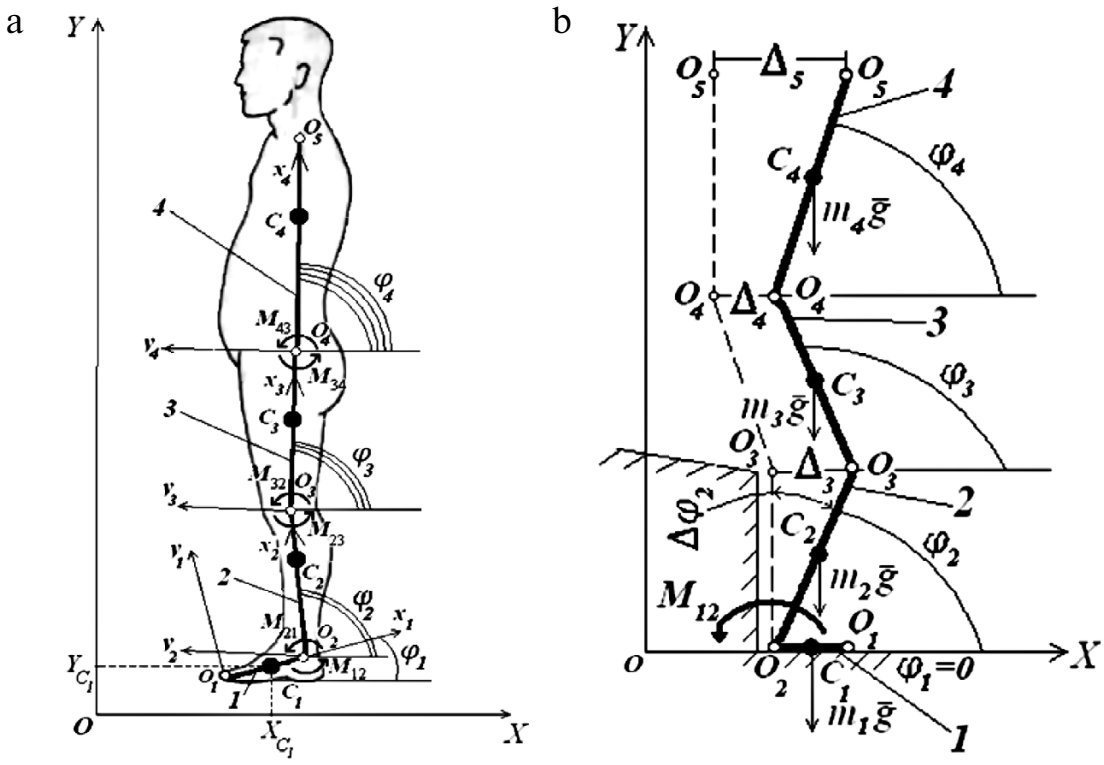

Fig. 1. Calculation diagram of the rehabilitation device.

elements of the system are rigid solid bodies; (ii) each of the links is represented by a rod of length l_i and mass m_i, concentrated in the symmetry center of the link C_i; (iii) counterclockwise direction is taken as positive rotation of the links.

For convenient description of kinematics of the multilink mechanism, four relative coordinate systems $O_ix_iy_i$ are used, whose orientation relative to the coordinate system OXY is defined by the angles φ_i (i = 1, ..., 4).

The movement of each link of the device is described by three generalized coordinates x_{Ci}, y_{Ci}, φ_i, where x_{Ci}, y_{Ci} are coordinates of the center of mass of the i-th link; φ_i is the angle of rotation of the i-th link relative to the horizontal axis.

Radius vectors of basic points of the links in the absolute coordinate system were determined using rotation matrices $T_{i,i-1}$ providing transformation of coordinates the systems $O_ix_iy_i$ to the systems $O_{i-1}x_{i-1}y_{i-1}$ [9].

The system of differential equations of motion of the device was written using Lagrange equations of the second kind:

$$\frac{d}{dt}\left(\frac{\partial T}{\partial \dot{q}_n}\right)-\frac{\partial T}{\partial q_n}=Q_n,$$

where T is the kinetic energy of the system; q_n in a generalized coordinate; Q_n is generalized force by the coordinate q_n.

The kinetic energy of the system is defined as the sum of the kinetic energies of all the bodies of the system, which, in turn, perform a plane motion. Wherein:

$$T_i = m_i\frac{\dot{x}_{Ci}^2+\dot{y}_{Ci}^2}{2}+\frac{I_{Ci}\dot{\varphi}_i^2}{2},$$

where $I_{Ci} = m_il_i^2/12$ are central moments of inertia of the units; $\dot{x}_{Ci}$, $\dot{y}_{Ci}$ are the projections of speeds centers of mass of the links on axes of the absolute coordinate system.

After appropriate transformations, the system of differential equations describing the motion of the four-link mechanism has the form shown in Fig. 2.

The generalized forces were determined using the principle of potential displacements (see Fig. 1b). At the initial time, the rehabilitation device was located on a patient in sitting position X_{C1}, Y_{C2}, φ_1, and there were certain relative angles φ_i between the links of the device. Next, the fourth link rotated in the clockwise direction under the action of the corresponding torque M_{43} (direct actuation). Upon reaching a certain

$$
\begin{cases}
\ddot{x}_{C1}\sum_{i=1}^{4} m_i - \ddot{\varphi}_1(m_2+m_3+m_4)\frac{l_1}{2}\sin\varphi_1 - \ddot{\varphi}_2(m_2+2m_3+2m_4)\frac{l_2}{2}\sin\varphi_2 - \ddot{\varphi}_3(m_3+m_4)\frac{l_3}{2}\sin\varphi_3 - \dot{\varphi}_1^2(m_2+m_3+m_4)\frac{l_1}{2}\cos\varphi_1 - \\
-\dot{\varphi}_2^2(m_2+2m_3+2m_4)\frac{l_2}{2}\cos\varphi_2 - \dot{\varphi}_3^2(m_3+2m_4)\frac{l_3}{2}\cos\varphi_3 - m_4\frac{l_4}{2}\ddot{\varphi}_4\sin\varphi_4 - m_4\frac{l_4}{2}\dot{\varphi}_4^2\cos\varphi_4 = Q_1; \\
\ddot{y}_{C1}\sum_{i=1}^{4} m_i + \ddot{\varphi}_1(m_2+m_3+m_4)\frac{l_1}{2}\cos\varphi_1 + \ddot{\varphi}_2(m_2+2m_3+2m_4)\frac{l_2}{2}\cos\varphi_2 + \ddot{\varphi}_3(m_3+m_4)\frac{l_3}{2}\cos\varphi_3 - \dot{\varphi}_1^2(m_2+m_3+m_4)\frac{l_1}{2}\sin\varphi_1 - \\
-\dot{\varphi}_2^2(m_2+2m_3+2m_4)\frac{l_2}{2}\sin\varphi_2 - \dot{\varphi}_3^2(m_3+2m_4)\frac{l_3}{2}\sin\varphi_3 + m_4\frac{l_4}{2}\ddot{\varphi}_4\cos\varphi_4 - m_4\frac{l_4}{2}\dot{\varphi}_4^2\sin\varphi_4 = Q_2; \\
\ddot{x}_{C1}(m_2+m_3+m_4)\frac{l_1}{2}\sin\varphi_1 + \ddot{y}_{C1}(m_2+m_3+m_4)\frac{l_1}{2}\cos\varphi_1 + \ddot{\varphi}_1\left[I_{C1}(m_2+m_3+m_4)\frac{l_1^2}{4}\right] + \ddot{\varphi}_1\left(\frac{m_2}{2}+m_3+m_4\right)\frac{l_1 l_2}{2}\cos(\varphi_2-\varphi_1) + \\
+\ddot{\varphi}_3\left(\frac{m_3}{2}+m_4\right)\frac{l_1 l_3}{2}\cos(\varphi_3-\varphi_1) + \ddot{\varphi}_4\frac{m_4}{2}\frac{l_1 l_4}{4}\cos(\varphi_4-\varphi_1) + \dot{\varphi}_2^2\left(\frac{m_2}{2}+m_3+m_4\right)\frac{l_1 l_2}{2}\sin(\varphi_1-\varphi_2) + \\
+\dot{\varphi}_3^2\left(\frac{m_3}{2}+m_4\right)\frac{l_1 l_3}{2}\sin(\varphi_1-\varphi_3) + \dot{\varphi}_4^2 m_4\frac{l_1 l_4}{4}\sin(\varphi_1-\varphi_4) = Q_3; \\
-\ddot{x}_{C1}(m_2+2m_3+2m_4)\frac{l_2}{2}\sin\varphi_2 + \ddot{y}_{C1}(m_2+2m_3+2m_4)\frac{l_2}{2}\cos\varphi_2 + \ddot{\varphi}_1\left(\frac{m_2}{2}+m_3+m_4\right)\frac{l_1 l_2}{2}\cos(\varphi_1-\varphi_2) + \\
+\ddot{\varphi}_2\left[I_{C2}+l_2^2\left(\frac{m_2}{4}+m_3+m_4\right)\right] + \ddot{\varphi}_3(m_3+2m_4)\frac{l_2 l_3}{2}\cos(\varphi_3-\varphi_2) + \ddot{\varphi}_4^2 m_4\frac{l_2 l_4}{2}\cos(\varphi_4-\varphi_2) + \\
+\dot{\varphi}_1^2\left(\frac{m_2}{2}+m_3+m_4\right)\frac{l_1 l_3}{2}\sin(\varphi_2-\varphi_1) + \dot{\varphi}_3^2(m_3+2m_4)\frac{l_2 l_3}{2}\sin(\varphi_2-\varphi_3) + \dot{\varphi}_4^2 m_4\frac{l_2 l_4}{2}\sin(\varphi_2-\varphi_4) = Q_4; \\
-\ddot{x}_{C1}(m_3+2m_4)\frac{l_3}{2}\sin\varphi_3 + \ddot{y}_{C1}(m_3+2m_4)\frac{l_3}{2}\cos\varphi_3 + \ddot{\varphi}_1(m_3+2m_4)\frac{l_1 l_3}{4}\cos(\varphi_1-\varphi_3) + \ddot{\varphi}_2(m_3+2m_4)\frac{l_2 l_3}{2}\cos(\varphi_2-\varphi_3) + \\
+\ddot{\varphi}_3\left(I_{C3}+m_3\frac{l_3^2}{4}+m_4 l_3^2\right) + \ddot{\varphi}_4^2 m_4\frac{l_3 l_4}{2}\cos(\varphi_4-\varphi_3) + \dot{\varphi}_1^2(m_3+2m_4)\frac{l_1 l_3}{4}\sin(\varphi_3-\varphi_1) + \dot{\varphi}_2^2(m_3+2m_4)\frac{l_2 l_3}{2}\sin(\varphi_3-\varphi_2) + \\
+\dot{\varphi}_4^2 m_4\frac{l_3 l_4}{2}\sin(\varphi_3-\varphi_4) = Q_5; \\
-\ddot{x}_{C1}m_4\frac{l_4}{2}\sin\varphi_4 + \ddot{y}_{C1}m_4\frac{l_4}{2}\cos\varphi_4 + \ddot{\varphi}_1 m_4\frac{l_1 l_4}{4}\cos(\varphi_1-\varphi_4) + \ddot{\varphi}_2 m_4\frac{l_2 l_4}{2}\cos(\varphi_2-\varphi_4) + \ddot{\varphi}_2 m_4\frac{l_2 l_4}{2}\cos(\varphi_2-\varphi_4) + \\
+\ddot{\varphi}_3^2 m_4\frac{l_3 l_4}{2}\cos(\varphi_3-\varphi_4) + \ddot{\varphi}_4\left(I_{C4}+m_4\frac{l_4^2}{4}\right) + \dot{\varphi}_1^2 m_4\frac{l_1 l_4}{4}\sin(\varphi_4-\varphi_1) + \dot{\varphi}_2^2 m_4\frac{l_2 l_4}{2}\sin(\varphi_4-\varphi_2) + \dot{\varphi}_3^2 m_4\frac{l_3 l_4}{2}\sin(\varphi_4-\varphi_3) = Q_6.
\end{cases}
$$

Fig. 2. System of differential equations describing movement of the four-link mechanism.

numerical value of the absolute angle φ_4^*, there was a transition to the next stage – straightening and takeoff of the third and fourth units from the support surface. In joint O_4 the direction of the M_{43} torque was reversed (reverse actuation), in joint O_3 the torque M_{32} acted, link 3 rotated clockwise; the counterclockwise torque M_{12} started acting joint O_2, connecting links 1 and 2.

To study the transfer of a patient from the sitting to a standing position, theoretical studies were conducted based on the analytical relationships (see Fig. 3) that determine the range of motion in various joints of the human lower limbs in the mode of rising from a chair for subsequent implementation in the design of the rehabilitation device.

The computational model of the multilink biomechatronic mechanotherapy device for rehabilitation of the human lower limb is based on solid models developed in the Pro/ENGINEER WF5 CAD system. In accordance with the calculation, kinematic parameters of the multilink system participating in a respective cycle were established. The rehabilitation device (Fig. 4) is a "two-legged" multiaxial mechanism driven by active joints with linear actuators that are given commands from the control system, and they simulate the operation of the lower limb muscles. Each "leg" of the device consists of three mobile units (foot, hip, shank) connected in series with rotational kinematic pairs between each. The legs are contacting the support surface via the surface of

the feet. The actuators of the active joints were installed using a scheme of double-arm levers (Fig. 4) that provide the required torque and angle characteristics at the same time. All the identical actuators are pivotally connected with the links of the rehabilitation device: one on the body, two on the hip, and one on the lower leg. The rod of each actuator is also pivotally connected to corresponding links of the device. Design parameters of the rehabilitation device are identical to average anthropometric parameters of a human patient: the length of the shank link l_2 = 0.4 m, the hip l_3 = 0.4 m, and the body l_2 = 0.5 m.

Values of the resulting torque of active joints of the hip, knee, and ankle of the rehabilitation device at the full elongation of the actuators are shown in Table 1.

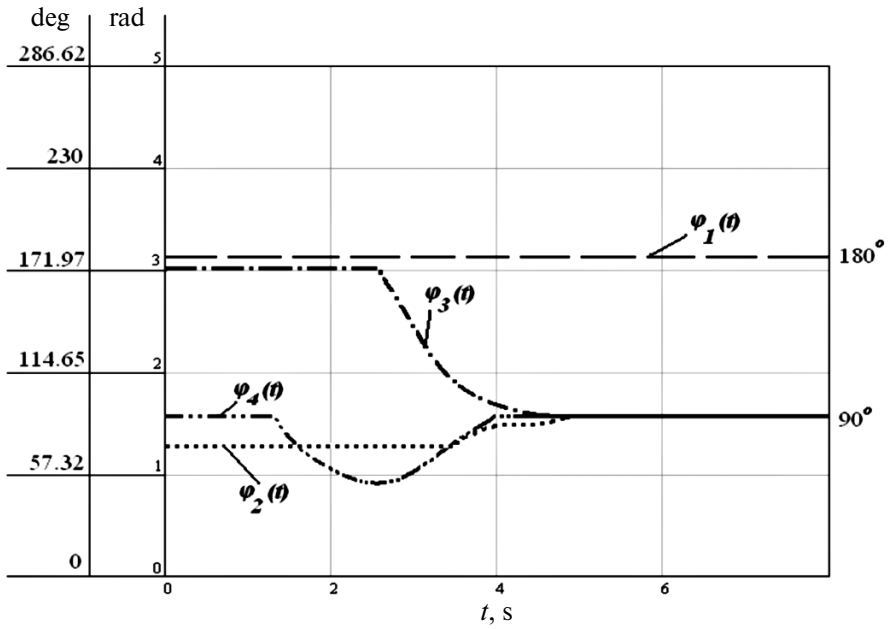

Fig. 3. Results of experimental study of range of motion (rotation angles) of links in the rising mode: 1) foot O_1O_2 – $\varphi_1(t)$; 2) shank O_2O_3 – $\varphi_2(t)$; 3) hip O_3O_4 – $\varphi_3(t)$; 4) body O_4O_5 – $\varphi_4(t)$.

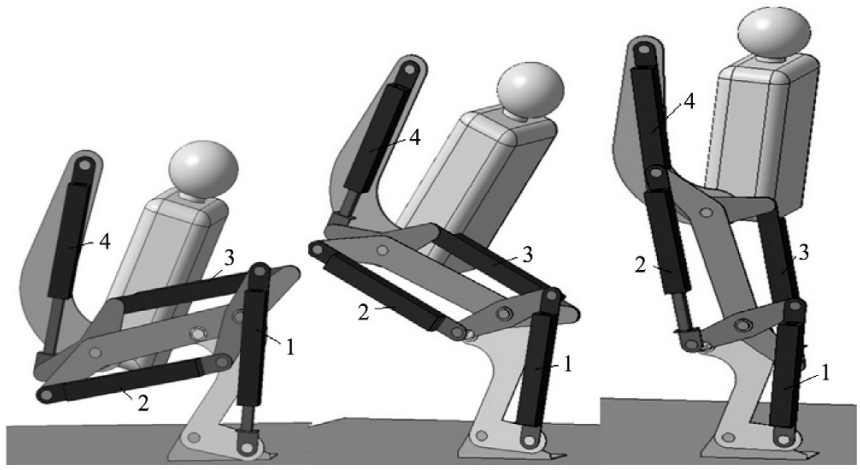

Fig. 4. Stages of functioning (three-dimensional model) of the rehabilitation device in the rising mode: 1) ankle joint actuator; 2) lower actuator of the knee joint; 3) upper actuator of the knee joint; 4) actuator of the hip joint.

Results

The results of the numerical simulation of dynamic processes taking place during functioning of the rehabilitation device were plotted using Mathcad software. The presentation of the results is most informative and enables visual estimation of changes of dynamic parameters of the device. Figure 5a presents the intermediate positions of the links of a planar mechanism when putting the patient in vertical position. Analysis of the charts reveals the fol-

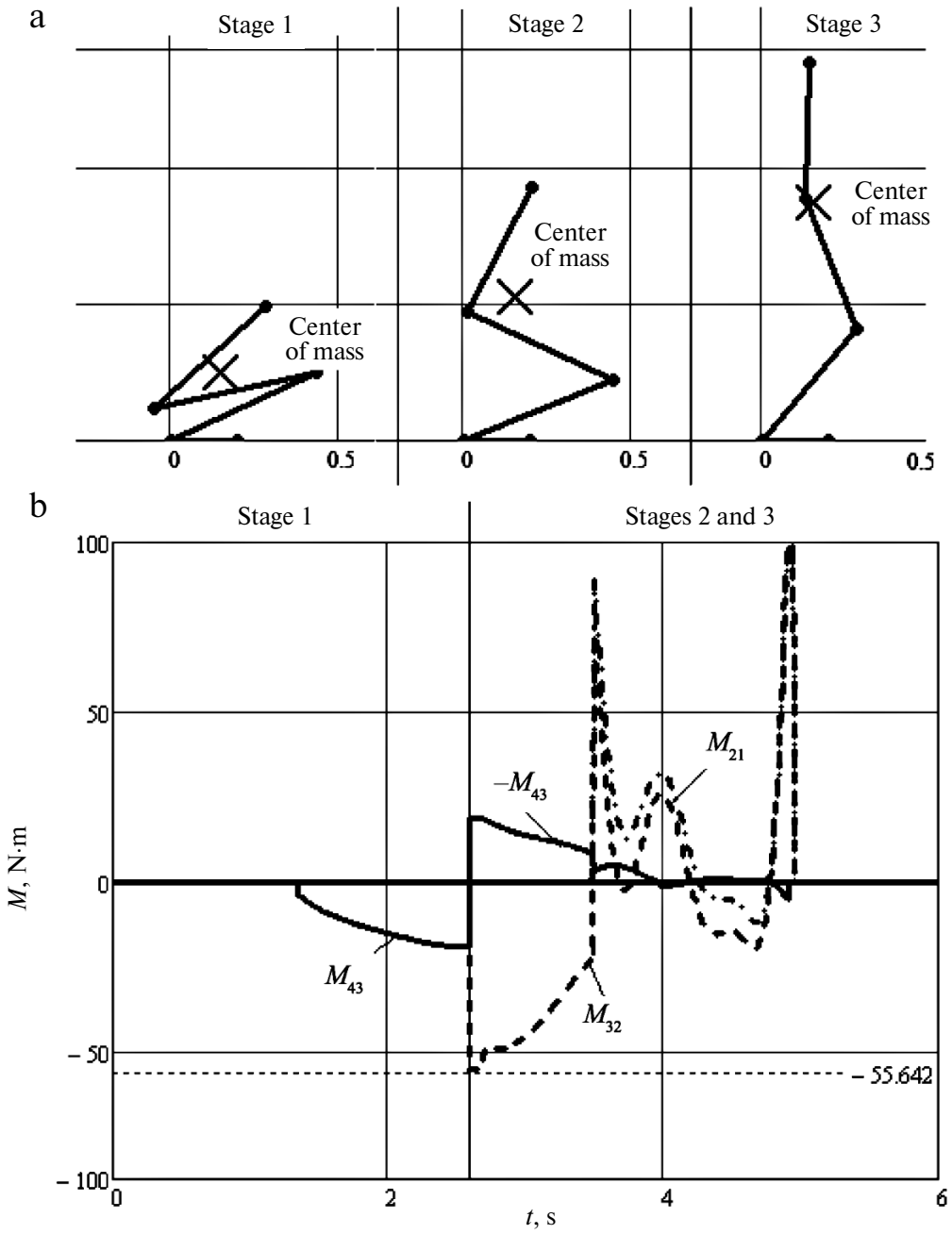

Fig. 5. Results of modeling the movement of units of the rehabilitation device: a) intermediate position of parts of the plane mechanism for the implementation of verticalization of the patient; b) diagrams of changes of the control torques occurring in the electroactuator elements of the active joints.

TABLE 1. Values of the Resulting Torques in the Joints

	Body tilted forward at an angle of 30°	Body tilted forward at an angle of 20°	Body tilted forward at an angle of 10°	Vertical position of the body
Ankle, N·m/mm	189/0	189/0	189/0	189/0
Hip joint, N·m/mm	169/100	157/150	132/200	166/50
		Knee joint		
Upper actuator, N·m/mm	170/100	162/150	140/200	163/50
Lower actuator, N·m/mm	132/200	132/200	132/200	132/200

lowing steps of motion: Stage 1 – beginning of the motion phase, the body is tilted forward ($90° < \varphi_4 < 50°$, $\varphi_3 = \text{const} = 173°$) to move the center of mass, the angle of the ankle is reduced by a small value ($70° < \varphi_4 < 66°$), which is caused by movement of the body; Stage 2 – the body takes off the support surface and gradually transitions to an upright position; Stage 3 – vertical position, all the angles except for the foot angle are equal to 90°. During motion, the center of mass is constantly moving along a certain complex trajectory. Therefore, from a mechanical point of view the motion of the links of the biomechatronic device can be regarded as changes in the conditions of equilibrium of forces (see Fig. 1b) that influence the multilink system, in turn leading to redistribution of stresses in the muscle groups of the lower extremities of the patient. Involuntary movement can change with the ratio of forces toward and away from equilibrium. The additional use of muscle force of the patient, especially in case of involuntary movements, can disturb the equilibrium of the system, which limits the possibilities of the device in implementing walking with dynamic stability. Figure 5b presents diagrams of changes of the control torques occurring in the electroactuator elements of the active joints in time for passive mode of rehabilitation, when the muscles of the lower limbs of the patient are not involved in the rising process. Peak values of torques in the knee (M_{32} = 55.6 N·m) and the hip (M_{43} = 24 N·m) joints are observed in the transition from stage 1 to stage 2, the peak values of the ankle joint (M_{21} = 100 N·m) is observed at the end of the stage 2, when the patient is almost in a vertical position. These parameters are explained by necessity to move the center of mass of the system to implement the given movement of the links in accordance with the identified stages of motion.

Conclusion

An originally multilink biomechatronic device for rehabilitation lower extremities in humans was developed based on translational motion modules [10]. This structure is designed to promote recovery of motor skills of patients suffering from paralysis of the legs, when teaching them to rise from a bed or a chair.

The study was financially supported by the Russian Science Foundation (grant No. 14-39-00008).

REFERENCES

1. Dimitrijevic M., Gerasimenko Yu., Pinter M., Ann. NY Acad. Sci., **860**, 360 (1998).
2. Gerasimenko Yu.P., Avelev V.D., Nikitin O.A., Ros. Fiziol. Zh. I.M. Sechenova, **87**, No. 9, 1164-1170 (2001).
3. Grigor'ev A.I., Kozlovskaia I.B., Shenkman B.S., Ros. Fiziol. Zh. I.M. Sechenova, **90**, No. 5, 508-521 (2004).
4. Moshonkin T.R., Gilerovich E.G., Fedorova E.A. et al., Bul. Exp. Biol. Med., **138**, No. 8, 225-229 (2004).
5. Alekhin A.I., Belen'kii V.E., Grishin A.A., Lenskii A.V., RF Patent 12352316.
6. Ivanov V.G., Merzanyukova E.V., RF Patent 2493805.
7. Jatsun S.F., Rukavitsyn A.N., Izv. Samar. Nauch. Centra RAN, **14**, No. 4(5), 1351-1354 (2012).
8. Jatsun S.M.., Rukavitsyn A.N., Med. Tekhn., No. 3, 38-41 (2015).
9. Vorob'ev E.I., Popov S.A., Sheveleva G.I., Mechanics of Industrial Robots. Book 1: Kinematics and Dynamics [in Russian], Vys. Shkola, Moscow (1988).
10. Jatsun S.F., Rukavitsyn A.N., Yakovlev I.A., RF Patent 134791.